Single-Particle Motion and Vortex Stretching in Three-Dimensional Turbulent Flows

Alain Pumir,[1,2,*] Haitao Xu,[2,3,†] Eberhard Bodenschatz,[2,4,5] and Rainer Grauer[6]
[1]Ecole Normale Supérieure de Lyon, 69007 Lyon, France
[2]Max Planck Institute for Dynamics and Self-Organization (MPIDS), 37077 Göttingen, Germany
[3]Center for Combustion Energy and Department of Thermal Engineering, Tsinghua University, 100084 Beijing, China
[4]Institute for Nonlinear Dynamics, University of Göttingen, 37077 Göttingen, Germany
[5]Laboratory of Atomic and Solid State Physics and Sibley School of Mechanical and Aerospace Engineering, Cornell University, Ithaca, New York 14853, USA
[6]Institute for Theoretical Physics I, Ruhr Universität Bochum, 44780 Bochum, Germany
(Received 26 November 2015; published 24 March 2016)

Three-dimensional turbulent flows are characterized by a flux of energy from large to small scales, which breaks the time reversal symmetry. The motion of tracer particles, which tend to lose energy faster than they gain it, is also irreversible. Here, we connect the time irreversibility in the motion of single tracers with vortex stretching and thus with the generation of the smallest scales.

DOI: 10.1103/PhysRevLett.116.124502

The generation of small scales, or large velocity gradients, is fundamental to three-dimensional (3D) turbulent fluid flows; it is responsible for a flux of energy ε from large to small scales. This flux makes turbulence a system very far from equilibrium, which differs fundamentally from other systems close to thermal equillibrium [1,2]. One of the seminal theoretical results in the limit of very small viscosity or very large Reynolds numbers [3,4] is that $\langle \Delta u(x)^3 \rangle = -\frac{4}{5}\varepsilon x$, where $\langle \Delta u(x)^3 \rangle$, is the third moment of the longitudinal velocity difference between two points separated by a distance x. This fundamental asymmetry in velocity differences persists all the way down to very small distances so the third moment of the velocity derivative $\partial_x u_x$ is *negative*: $\langle (\partial_x u_x)^3 \rangle \leq 0$. In fact, in the case of homogeneous and isotropic turbulent flows, which we are focusing on here, the third moment of $\partial_x u_x$ is related to the generation of the smallest scales in turbulence through the amplification of vorticity $\omega = \nabla \times \mathbf{u}$. Vortex stretching, the rate of growth of $\frac{1}{2}\langle \omega^2 \rangle$, is found from the Navier-Stokes equations to be $\langle \omega \cdot \mathbf{S} \cdot \omega \rangle$, where $S_{ij} = (\partial_j u_i + \partial_i u_j)/2$ represents the rate of strain of the flow [5,6]. This term reduces to $\langle \omega \cdot \mathbf{S} \cdot \omega \rangle = -\frac{35}{6}\langle (\partial_x u_x)^3 \rangle$ [7], so $\langle (\partial_x u_x)^3 \rangle < 0$ is equivalent to the generation (stretching) of vorticity: $\langle \omega \cdot \mathbf{S} \cdot \omega \rangle > 0$.

Recently, it was shown that the motion of individual tracer particles, which follow the flow, is irreversible: Tracers tend to lose kinetic energy faster than they gain it [8]. This implies negative odd order moments of the kinetic energy increment between two different times along a trajectory, and in particular, of the rate of change of kinetic energy, which is equal to the power p of the forces acting on particles. Our construction is based on decomposing the power p into a local part p_L, due to the change of flow field with time at fixed positions, and a convective part p_C, which accounts for the change of kinetic energy when a particle is moving in an otherwise frozen flow field. Here, we present evidence that the origin of this irreversibility [8–12] lies in the generation of the smallest scales of the flow. With analytic calculation and support from numerical simulations we connect vortex stretching, or, equivalently, the generation of small scales, to the third moment $\langle p^3 \rangle$ along individual tracer trajectories.

Analytical results: Vortex stretching and tracer particle motion in turbulence.— Our analytic work is based on the observation that the rate of change of kinetic energy of a tracer particle moving along a streamline of the flow, or equivalently, along the trajectory in a frozen turbulent velocity field, $p_C = \mathbf{u} \cdot (\mathbf{u} \cdot \nabla \mathbf{u})$, reduces to the simple form: $p_C = \mathbf{u} \cdot \mathbf{S} \cdot \mathbf{u}$. In any flow, the straining $\mathbf{S}$ decomposes into a superposition of compression or stretching along three orthogonal directions, denoted by $\mathbf{e}_i$, with three straining rates, λ_i. The vectors $\mathbf{e}_i$ and the straining rates λ_i are the eigenvectors and eigenvalues of $\mathbf{S}$. A positive (negative) value of λ_i corresponds to stretching (compression) in the direction $\mathbf{e}_i$. Incompressibility (i.e., volume conservation) imposes that $\lambda_1 + \lambda_2 + \lambda_3 = 0$: i.e., the amounts of stretching and compression along the three directions $\mathbf{e}_i$ sum up to 0. In a turbulent flow, the velocity field $\mathbf{u}$ and the rate of strain $\mathbf{S}$ are expected to be independent of each other. This is a consequence of the fact that $\mathbf{u}$ is controlled by the large scales of the flow, whereas $\mathbf{S}$ is controlled by the small scales. In a highly turbulent flow, these scales are vastly different, so $\mathbf{u}$ and $\mathbf{S}$ are only very weakly coupled. Under these conditions, which we will show later to be satisfied, the third moment of p_C can be simply related to the average $\langle \mathrm{tr}(\mathbf{S}^3) \rangle$:

$$\langle p_C^3 \rangle = \langle (\mathbf{u} \cdot \mathbf{S} \cdot \mathbf{u})^3 \rangle = \frac{8}{105}\langle |\mathbf{u}|^6 \rangle \langle \mathrm{tr}(\mathbf{S}^3) \rangle. \quad (1)$$

To prove Eq. (1), we project the velocity $\mathbf{u}$ in the eigenframe $\mathbf{e}_i$ of the rate of strain $\mathbf{S}$. Denoting $\hat{x}_i$, the

cosines of the angles between the velocity $\mathbf{u}$ and the unit vectors $\mathbf{e}_i$: $\hat{x}_i \equiv \mathbf{u}\cdot\mathbf{e}_i/|\mathbf{u}| = u_i/|\mathbf{u}|$, the expression of $\mathbf{u}\cdot\mathbf{S}\cdot\mathbf{u}$ reduces to

$$\mathbf{u}\cdot\mathbf{S}\cdot\mathbf{u} = \sum_{i=1}^{3}\lambda_i u_i^2 = \mathbf{u}^2\sum_{i=1}^{3}\lambda_i\hat{x}_i^2. \quad (2)$$

The independence between $\mathbf{u}$ and $\mathbf{S}$ implies that the three cosines $\hat{x}_i$ define a point that is uniformly distributed on the unit sphere in three dimensions, which allows us to evaluate geometrical quantities such as $\langle\hat{x}_i^6\rangle = 1/7$, $\langle\hat{x}_1^2\hat{x}_2^4\rangle = 1/35$, and $\langle\hat{x}_1^2\hat{x}_2^2\hat{x}_3^2\rangle = 1/105$. Using also the identity $\langle\mathrm{tr}(\mathbf{S}^3)\rangle = 3\langle\lambda_1\lambda_2\lambda_3\rangle$ readily leads to Eq. (1). We further notice that the average $\langle\mathrm{tr}(\mathbf{S}^3)\rangle$ is in fact related, in statistically homogeneous turbulent flows, to vortex stretching $\langle\omega\cdot\mathbf{S}\cdot\omega\rangle$, via the following relation [7]:

$$\langle\omega\cdot\mathbf{S}\cdot\omega\rangle = -\frac{4}{3}\langle\mathrm{tr}(\mathbf{S}^3)\rangle. \quad (3)$$

Therefore, combining Eqs. (1) and (3), we obtain

$$\langle p_C^3\rangle = \frac{8}{105}\langle|\mathbf{u}|^6\rangle\langle\mathrm{tr}(\mathbf{S}^3)\rangle = -\frac{2}{35}\langle|\mathbf{u}|^6\rangle\langle\boldsymbol{\omega}\cdot\mathbf{S}\cdot\boldsymbol{\omega}\rangle. \quad (4)$$

It has been noticed many times that the probability distributions of individual components of velocity $\mathbf{u}$ are close to Gaussian [13,14]. Assuming a Gaussian distribution of $\mathbf{u}$ allows us to express the 6th moment of velocity in Eq. (4) in terms of the velocity variance $\langle\mathbf{u}^2\rangle$. This variance can be expressed in terms of the viscosity ν, the dissipation ε, and the Taylor-microscale Reynolds number, R_λ, which characterizes the intensity of turbulence $\langle\mathbf{u}^2\rangle = \sqrt{(3/5)}R_\lambda(\nu\varepsilon)^{1/2}$. Last, using the relation between $\langle\mathrm{tr}(\mathbf{S}^3)\rangle$ and the skewness of the velocity derivative $S_{\partial_x u_x} = \langle(\partial_x u_x)^3\rangle/\langle(\partial_x u_x)^2\rangle^{(3/2)} = \langle(\partial_x u_x)^3\rangle/(\varepsilon/15\nu)^{3/2}$ [7], Eq. (4) leads to

$$\langle p_C^3\rangle = \frac{7}{225}S_{\partial_x u_x}R_\lambda^3\varepsilon^3. \quad (5)$$

Equations (4) and (5) were obtained analytically, and provide a quantitative relation between vortex stretching and the kinetic energy change along a streamline, or equivalently, the rate of kinetic energy change in a "frozen," i.e., time independent, turbulent flow field. The same assumptions of lack of correlation between $\mathbf{u}$ and $\mathbf{S}$, and of a Gaussian distribution of the velocity $\mathbf{u}$, also lead to an exact determination of the variance of p_C:

$$\langle p_C^2\rangle = \frac{1}{15}R_\lambda^2\varepsilon^2. \quad (6)$$

We further notice that the total rate of kinetic energy change along a particle trajectory in a turbulent flow, i.e., the instantaneous power of the forces acting on the fluid particle, $p = (d/dt)(\frac{1}{2}\mathbf{u}^2) = \mathbf{a}\cdot\mathbf{u} = \mathbf{u}\cdot\partial_t\mathbf{u} + \mathbf{u}\cdot(\mathbf{u}\cdot\nabla\mathbf{u})$, decomposes into the *convective* contribution $p_C = \mathbf{u}\cdot\mathbf{S}\cdot\mathbf{u}$, which we investigated above, plus an additional *local* contribution p_L due to the time variation of $\mathbf{u}$: $p_L = \mathbf{u}\cdot\partial_t\mathbf{u}$. To rigorously establish a relation between vortex stretching and the Lagrangian quantity p, one needs to also consider the properties of p_L. We recall that in this context the third moment of p is also negative [8], i.e., has the same sign as $\langle p_C^3\rangle$ in 3D turbulent flows.

Decomposition of the power p: Numerical results.— To proceed, we rely on numerical results, based on the determination of the motion of tracer particles in homogeneous and isotropic 3D turbulent flows, using fully resolved direct numerical simulations (DNS). Two simulations were generated by using the cluster at ENS Lyon; see Ref. [15]. Additionally, we used data from the Johns Hopkins University database [16].

In homogeneous and stationary flows, the first moments of p, p_C, and p_L are all exactly 0. The magnitudes of p_C and p_L may be estimated from simple dimensional arguments: $|p_C| \sim |p_L| \sim U^2/\tau_K$, where U is the typical size of the velocity fluctuations, and τ_K is the shortest time scales of the turbulent eddies. Using the known relation $\tau_K \sim (U^2/\varepsilon)/R_\lambda$ [5,6], one finds $|p_C| \sim |p_L| \sim \varepsilon R_\lambda$. Note that this simple scaling of p_C is consistent with Eq. (6). Our numerical results, shown in Table I, support these scalings.

The growth of the variance of p/ε as $R_\lambda^{4/3}$ found in Ref. [8] thus points to a cancellation between p_L and p_C. Table I shows that the correlation coefficient between p_L and p_C: $\langle p_C p_L\rangle/(\langle p_C^2\rangle\langle p_L^2\rangle)^{1/2}$, is approximately -0.9 and approaches -1 as the Reynolds number increases. This anticorrelation results in the variance of p to be much smaller than those of p_C and p_L. Although reminiscent of the well-documented cancellation between the acceleration components $\mathbf{a}_C = \mathbf{u}\cdot\nabla\mathbf{u}$ and $\mathbf{a}_L = \partial_t\mathbf{u}$ [17–20], the cancellation between p_C and p_L *cannot* be simply deduced from the results of Refs. [18,19]. Please note that p_C and p_L involve the projections of $\mathbf{a}_C$ and $\mathbf{a}_L$ along the direction of the velocity $\mathbf{u}$, which is correlated with $\mathbf{a}$ [21].

Prevalence of vortex stretching on the third moment of p.—We now establish that the third moment $\langle p^3\rangle$ is dominated by $\langle p_C^3\rangle$. Figure 1 shows the joint probability

TABLE I. Second moments of the distributions of p/ε, p_C/ε, and p_L/ε at the three Reynolds numbers studied in this article. The values of β are measured from fitting the conditional averages $\langle p_L|p_C\rangle = -\beta p_C$.

R_λ	193	275	430
$\langle p^2\rangle/\varepsilon^2$	3.83×10^2	7.36×10^2	1.32×10^3
$\langle p_C^2\rangle/\varepsilon^2$	2.15×10^3	5.00×10^3	1.20×10^4
$\langle p_L^2\rangle/\varepsilon^2$	1.78×10^3	4.25×10^3	1.07×10^4
$-\langle p_L p_C\rangle/\varepsilon^2$	1.77×10^3	4.26×10^3	1.07×10^4
$\langle p_C p_L\rangle/(\langle p_C^2\rangle\langle p_L^2\rangle)^{1/2}$	-0.90	-0.92	-0.94
β	0.83	0.86	0.90

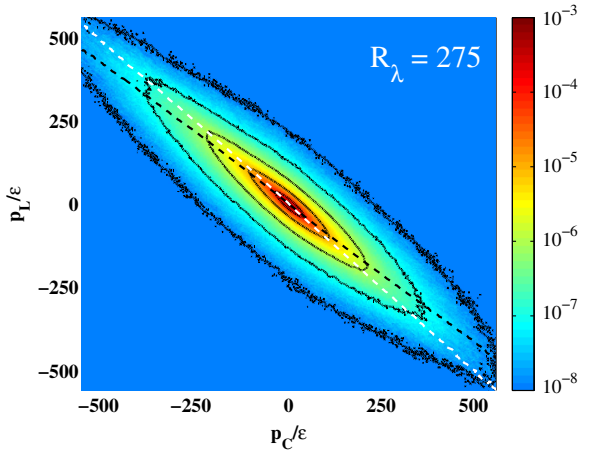

FIG. 1. The joint probability density function (PDF) between p_C/ε (horizontal) and p_L/ε (vertical) at $R_\lambda = 275$, color coded in a logarithmic scale. Equal-probability contours, separated by factors of 10, are shown. The black dashed line shows $\langle p_L|p_C\rangle/\varepsilon$, which is approximately $-0.86 \times p_C/\varepsilon$. The white dashed line shows $\langle p_C|p_L\rangle/\varepsilon$, which is approximately $-p_L/\varepsilon$.

distribution function (PDF) of p_C and p_L and indicates that the values of p_C and p_L cluster close to the line $p_C + p_L = 0$, thus implying a cancellation between the two quantities, which increases with R_λ. Our numerical simulations reveal an approximately linear relation between the conditional average $\langle p_L|p_C\rangle$ and p_C (shown as the black dashed line in Fig. 1): $\langle p_L|p_C\rangle \approx -\beta(R_\lambda)p_C$. The dimensionless coefficient β, shown in Table I, increases weakly with R_λ, which is consistent with the observed tendency of p_L and p_C to become increasingly anticorrelated when R_λ increases. Consistent with $\langle p_L|p_C\rangle \approx -\beta p_C$, we observe that the following relations,

$$\langle p_L p_C\rangle = -\beta\langle p_C^2\rangle \quad \text{and} \quad \langle p_L p_C^2\rangle = -\beta\langle p_C^3\rangle, \tag{7}$$

are numerically very accurately satisfied. These observations imply that $\langle p|p_C\rangle \approx (1-\beta)p_C$, where the coefficient $1-\beta$ decreases as R_λ increases, from $\approx$0.17 at $R_\lambda = 193$ to $\approx$0.10 at $R_\lambda = 430$. In comparison, the average of p_C conditioned on p_L, shown as the white dashed line in Fig. 1 is almost exactly equal to $-p_L$, which implies that $\langle p|p_L\rangle \approx 0$.

Figure 2 shows the joint PDFs of p_C and p (a) and of p_L and p (b). The conditional averages $\langle p|p_C\rangle$ and $\langle p|p_L\rangle$ are shown as black dashed lines. The conditional averages $\langle p_C|p\rangle$ and $\langle p_L|p\rangle$, shown as white dashed lines, have the particularly simple forms $\langle p_C|p\rangle \approx p$ and $\langle p_L|p\rangle \approx 0$. In addition, the joint PDF of p and p_L is almost symmetrical to both $p = 0$ and $p_L = 0$. The power p is therefore well correlated with p_C, but not with p_L. The lack of correlation between p on p_L, implies that

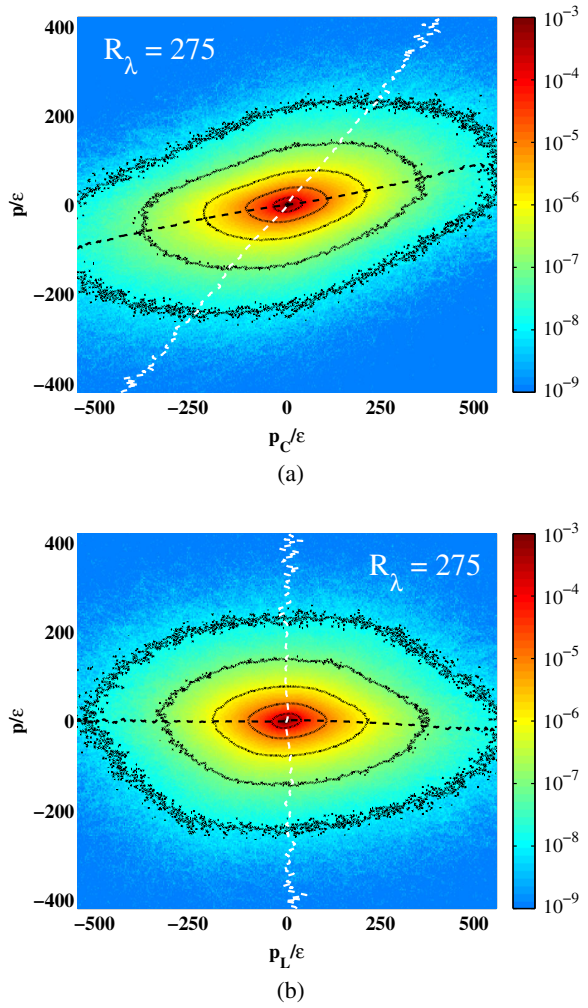

FIG. 2. (a) The joint PDF between p_C/ε (horizontal) and p/ε (vertical), and (b) the joint PDF between p_L/ε (horizontal) and p/ε (vertical), all at $R_\lambda = 275$, color coded in a logarithmic scale (see color bar). The equal-probability contours shown are separated by factors of 10. In (a), the black dashed line represents the conditional average $\langle p/\varepsilon|p_C/\varepsilon\rangle$, and is very close to $\langle p|p_C\rangle/\varepsilon \approx 0.14 \times p_C/\varepsilon$. The white dashed line corresponds to $\langle p_C/\varepsilon|p/\varepsilon\rangle$, and is well approximated by $\langle p_C|p\rangle/\varepsilon \approx p/\varepsilon$. In (b), the black dashed line represents the conditional average $\langle p/\varepsilon|p_L/\varepsilon\rangle$, and is very close to $\langle p|p_L\rangle/\varepsilon \approx 0$. The white dashed line indicates $\langle p_L/\varepsilon|p/\varepsilon\rangle$, and is also very well approximated by $\langle p_L|p\rangle/\varepsilon \approx 0$.

$$\langle p p_L\rangle \approx \langle p^2 p_L\rangle \approx \langle p p_L^2\rangle \approx 0. \tag{8}$$

Equations (7) and (8) lead to the relation $\langle p_L^2\rangle = \beta\langle p_C^2\rangle$ for the second moment, which also leads to

$$\langle p^2\rangle = (1-\beta)\langle p_C^2\rangle, \tag{9}$$

a relation which is numerically very accurately satisfied. We observe that the relation $\langle p_L^2\rangle = \beta\langle p_C^2\rangle$ is consistent with the expected scaling $p_L \sim \varepsilon R_\lambda$. Similarly, assuming

TABLE II. Third moments of the distributions of p/ε, p_C/ε, and p_L/ε at the three Reynolds numbers studied in this article.

R_λ	193	275	430
$-\langle p^3\rangle/\varepsilon^3$	3.87×10^3	1.23×10^4	3.21×10^4
$-\langle p_C^3\rangle/\varepsilon^3$	5.39×10^4	2.40×10^5	1.00×10^6
$\langle p_C^2 p_L\rangle/\varepsilon^3$	4.54×10^4	2.05×10^5	8.99×10^5
$-\langle p_C p_L^2\rangle/\varepsilon^3$	4.02×10^4	1.84×10^5	8.29×10^5
$\langle p_L^3\rangle/\varepsilon^3$	3.44×10^4	1.63×10^5	7.63×10^5
$\langle p^3\rangle/\langle p_C^3\rangle$	0.072	0.051	0.032

Eqs. (7) and (8) to be exact leads to the following relations between the third moments of p_C and p_L: $\langle p_L^3\rangle = -\beta\langle p_C^3\rangle$ and $\langle p_L^2 p_C\rangle = \beta\langle p_C^3\rangle$, leading to

$$\langle p^3\rangle = (1-\beta)\langle p_C^3\rangle. \tag{10}$$

This expression supports our claim that the assumption of independence between p and p_L imposes that the sign of $\langle p^3\rangle$ is given by $\langle p_C^3\rangle$.

We note that Eq. (9), together with the observed scaling $\langle p^2\rangle \propto R_\lambda^{4/3}$ and $\langle p_C^2\rangle \propto R_\lambda^2$, suggest that $(1-\beta)\propto R_\lambda^{-2/3}$. Equation (10) for $\langle p^3\rangle$ therefore implies that $\langle p^3\rangle \propto R_\lambda^{7/3}$, at odds with the experimental findings [8]. In fact, the relations above for the third moment are quantitatively inaccurate, as shown in Table II. We found that $\langle p_L^2 p\rangle$ is of the order of 10% of $|\langle p_C^3\rangle|$, much larger than predicted by Eq. (8) (in comparison, $\langle p_L p^2\rangle$ is found to be much smaller). To take the effect of nonzero $\langle p_L^2 p\rangle$ into account, we introduce $\zeta = \langle p_L^2 p\rangle/\langle p_C^3\rangle$, where ζ is a positive number of order $\sim$0.1 and decreases when R_λ increases. This then leads to $\langle p_L^2 p_C\rangle = (\beta-\zeta)\langle p_C^3\rangle$ and $\langle p_L^3\rangle = -(\beta-2\zeta)\langle p_C^3\rangle$, and, using Eq. (4), to

$$\begin{aligned}\langle p^3\rangle &= (1-\beta-\zeta)\langle p_C^3\rangle \\ &= -\frac{2}{35}(1-\beta-\zeta)\langle|\mathbf{u}|^6\rangle\langle\boldsymbol{\omega}\cdot\mathbf{S}\cdot\boldsymbol{\omega}\rangle,\end{aligned} \tag{11}$$

which shows first the direct dependence of $\langle p^3\rangle$ on $\langle p_C^3\rangle$, and second, relates it to vortex stretching via Eq. (4).

Using the dependence $\langle p_C^3\rangle \propto R_\lambda^3$, the observation $\langle p^3\rangle \approx -\varepsilon^3 R_\lambda^2$ [8], and Eq. (11) leads to $1-\zeta/(1-\beta)\propto R_\lambda^{-1/3}$. Our numerical results indeed indicate a slight decrease of $1-\zeta/(1-\beta)$, from 0.36 to 0.34, when R_λ increases from 193 to 430.

Lack of correlation between strain and velocity.— We reconsider now the essential assumption that $\mathbf{u}$ and $\mathbf{S}$ are uncorrelated. In the following, we sort the eigenvalues of $\mathbf{S}$, λ_i, in decreasing order: $\lambda_1 \geq \lambda_2 \geq \lambda_3$. Figure 3 shows that the PDFs of $|\hat{x}_i| = |\mathbf{e}_i\cdot\mathbf{e}_u|$, the absolute value of the cosine of the angle between the eigenvector $\mathbf{e}_i$ and the unit vector in the direction of the velocity $\mathbf{e}_u = \mathbf{u}/|\mathbf{u}|$ (the sign of this cosine is immaterial) at $R_\lambda = 275$, are approximately equal to 1. Figure 4 shows that the dependence of the conditional

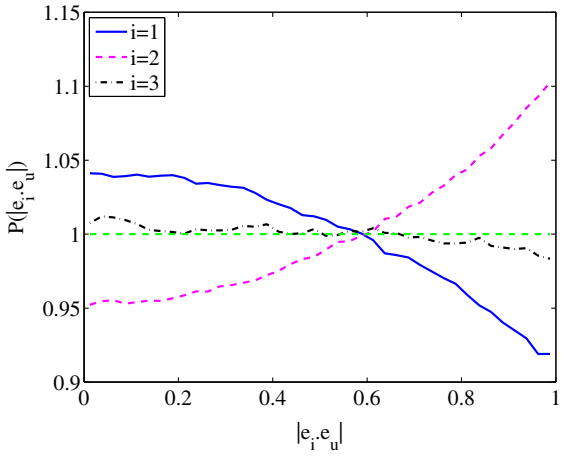

FIG. 3. The PDFs of the cosines of the angles between the direction of the velocity $\mathbf{u}$, and the eigenvectors $\mathbf{e}_i$ of $\mathbf{S}$ at $R_\lambda = 275$. The deviations of the PDF of $|\mathbf{e}_i\cdot\mathbf{e}_u|$ from the constant value 1 are weak, supporting the assumption of a lack of correlation between $\mathbf{u}$ and $\mathbf{S}$.

average of the eigenvalues of $\mathbf{S}$ on $\mathbf{u}^2$, $\langle\lambda_i|\mathbf{u}^2\rangle$, is weak, up to $2.5\langle\mathbf{u}^2\rangle$. As the probability of large values of $\mathbf{u}^2$ drops very rapidly when $\mathbf{u}^2$ increases [13,14,22], the stronger dependence of λ_i at higher values of $\mathbf{u}^2$ has only little effect on the low-order moments of p_C studied here. This justifies the assumption, used to derive Eqs. (4), (5), that $\mathbf{u}$ and $\mathbf{S}$ are uncorrelated.

Discussion.— In conclusion, using the physically justified approximation that velocity $\mathbf{u}$ and strain $\mathbf{S}$ are uncorrelated, we established that the third moment of p_C, the rate of change of kinetic energy along trajectories in a frozen velocity field reflects vortex stretching, and ultimately small scale generation in 3D turbulent flows. In particular, the *negative* sign of $\langle p_C^3\rangle$ originates from the *positive* sign of the vortex stretching. This main finding

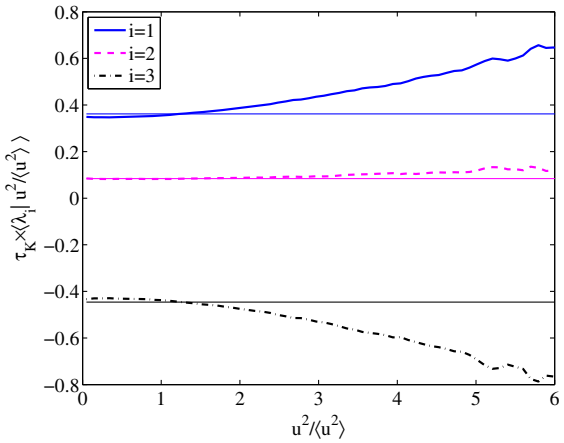

FIG. 4. The thick lines show the conditional averages of the eigenvalues of $\mathbf{S}$, $\langle\lambda_i|\mathbf{u}^2\rangle$, made dimensionless by $\tau_K = 1/(2\langle\mathbf{S}^2\rangle)^{1/2}$. The thin lines with the same color are the corresponding unconditional averages $\langle\lambda_i\rangle$, all at $R_\lambda = 275$.

relates to the recent observation concerning the third moment of the fluctuations of power p of fluid tracers along Lagrangian trajectories, which was observed to be negative [8]: $\langle p^3 \rangle \propto -\epsilon^3 R_\lambda^2$. Our result provides an essential step towards an exact relation between energy flux or small scale generation and Lagrangian single-particle statistics.

We note that in 2D turbulence, although the properties of the third moments of p are very similar to those in three dimensions [8], the approach proposed here does *not* apply, because of the entirely different mechanism of amplification of the large velocity gradient [23]. This leaves open the relation between the various fluxes and irreversibility in 2D flow, or in other flows of geophysical interest. The dynamics of inertial particles that have a significant density difference compared to the fluid, or have a significant size, involves completely different physical mechanisms [24–26]. It would be interesting to extend our analysis to such particles.

We thank G. Falkovich for insightful comments. This work is supported by the Max-Planck Society. A. P. acknowledges partial support from ANR (contract TEC 2), the Humboldt Foundation, and the PSMN at the Ecole Normale Supérieure de Lyon. R. G. acknowledges support from the German Research Foundation (DFG) through the program FOR 1048.

*alain.pumir@ens-lyon.fr
†hxu@tsinghua.edu.cn

[1] L. Onsager, Phys. Rev. **37**, 405 (1931).
[2] U. Seifert, Rep. Prog. Phys. **75**, 126001 (2012).
[3] A. N. Kolmogorov, Dokl. Akad. Nauk SSSR **30**, 301 (1941).
[4] G. Falkovich, K. Gawedzki, and M. Vergassola, Rev. Mod. Phys. **73**, 913 (2001).
[5] H. Tennekes and J. L. Lumley, *A First Course in Turbulence* (MIT Press, Cambridge, MA and London, England, 1972).
[6] U. Frisch, *Turbulence: The Legacy of A. N. Kolmogorov* (Cambridge University Press, Cambridge, Cambridge, England, 1995).
[7] R. Betchov, J. Fluid Mech. **1**, 497 (1956).
[8] H. Xu, A. Pumir, G. Falkovich, E. Bodenschatz, M. Shats, H. Xia, N. Francois, and G. Boffetta, Proc. Natl. Acad. Sci. USA **111**, 7558 (2014).
[9] G. Falkovich and A. Frishman, Phys. Rev. Lett. **110**, 214502 (2013).
[10] E. Leveque and A. Naso, Europhys. Lett. **108**, 54004 (2014).
[11] A. Pumir, H. Xu, G. Boffetta, G. Falkovich, and E. Bodenschatz, Phys. Rev. X **4**, 041006 (2014).
[12] T. Grafke, A. Frishman, and G. Falkovich, Phys. Rev. E **91**, 043022 (2015).
[13] G. Falkovich and V. Lebedev, Phys. Rev. Lett. **79**, 4159 (1997).
[14] M. Wilczek, A. Daitche, and R. Friedrich, J. Fluid Mech. **676**, 191 (2011).
[15] J. Jucha, H. Xu, A. Pumir, and E. Bodenschatz, Phys. Rev. Lett. **113**, 054501 (2014).
[16] Y. Li, E. Perlman, M. Wan, Y. Yang, C. Meneveau, R. Burns, S. Chen, A. Szalay, and G. Eyink, J. Turbul. **9**, N31 (2008).
[17] H. Tennekes, J. Fluid Mech. **67**, 561 (1971).
[18] A. Tsinober, P. Vedula, and P. K. Yeung, Phys. Fluids **13**, 1974 (2001).
[19] G. Gulitski, M. Kholmyansky, W. Kinzelbach, B. Lüthi, A. Tsinober, and S. Yorish, J. Fluid Mech. **589**, 83 (2007).
[20] O. Kamps, R. Friedrich, and R. Grauer, Phys. Rev. E **79**, 066301 (2009).
[21] A. M. Crawford, N. Mordant, and E. Bodenschatz, Phys. Rev. Lett. **94**, 024501 (2005).
[22] T. Gotoh, D. Fukayama, and T. Nakano, Phys. Fluids **14**, 1065 (2002).
[23] G. Boffetta and R. E. Ecke, Annu. Rev. Fluid Mech. **44**, 427 (2012).
[24] J. K. Eaton and J. R. Fessler, Int. J. Mutliphase Flows. **20**, 169 (1994).
[25] N. M. Qureshi, M. Bourgoin, C. Baudet, A. Cartellier, and Y. Gagne, Phys. Rev. Lett. **99**, 184502 (2007).
[26] G. P. Bewley, E. W. Saw, and E. Bodenschatz, New J. Phys. **15**, 083051 (2013).